A Critical Assessment of Methods for the Intrinsic Analysis of Liquid Interfaces: 2. Density Profiles

*Miguel Jorge**[†], *György Hantal*[‡], *Pál Jedlovszky*[‡,¥,¶], *and M. Natália D. S. Cordeiro*[§]

[†]LSRE/LCM – Laboratory of Separation and Reaction Engineering, Faculdade de Engenharia da Universidade do Porto, Rua Dr. Roberto Frias, 4200-465 Porto, Portugal

[‡]Laboratory of Interfaces and Nanosize Systems, Institute of Chemistry, Eotvos Loránd University, Pázmány Péter stny. 1/a, H-1117 Budapest, Hungary

[¥]HAS Research Group of Technical Analytical Chemistry, Gellért tér 4, H-1111 Budapest, Hungary

[¶]EKF Department of Chemistry, H-3300 Eger, Leanyka u. 6, Hungary

[§]REQUIMTE, Faculdade de Ciências da Universidade do Porto, Rua do Campo Alegre, 687, 4169-007 Porto, Portugal

Email address: mjorge@fe.up.pt

Title Running Head: Intrinsic Analysis of Liquid Interfaces

Abstract

Substantial improvements in the molecular level understanding of fluid interfaces have recently been achieved by recognizing the importance of detecting the *intrinsic* surface

of the coexisting condensed phases in computer simulations (i.e., after the removal of corrugations caused by capillary waves), and by developing several methods for identifying the molecules that are indeed located at the boundary of the two phases. In our previous paper [*J. Phys. Chem. C*, **2010**, *114*, 11169] we critically compared those methods in terms of reliability, robustness and computation speed. Once the intrinsic surface of a given phase is detected, various profiles, such as the density profiles of the components, can be calculated *relative to this intrinsic surface* rather than to the macroscopically planar Gibbs dividing surface. As a continuation of our previous study, here we present a detailed and critical comparison of various methods that can be used to calculate intrinsic density profiles once the full set of truly interfacial molecules has been identified. Two of the methods – the Fourier function and the Voronoi tessellation – are already described in the literature, two other methods – the covering surface and the triangular interpolation – are newly proposed algorithms, while one of them – the modified GIP method – is an improvement over an existing procedure. The different methods are again compared in terms of accuracy and computational cost. Based on this comparison we propose a fast and accurate protocol to be routinely used for intrinsic surface analyses in computer simulations.

Key words: Water/organic interfaces, Intrinsic profiles, Statistical Mechanics, Molecular Simulation.

1. Introduction

Gas-liquid and liquid-liquid interfaces are the subject of significant interest from the scientific community, playing an important role in several chemical, physical, biological and environmental processes [1,2]. Recent advances in cutting-edge experimental techniques [1,3] and computational methods [2] have dramatically enhanced our fundamental knowledge of the molecular-level structure and properties of liquid interfaces. The analysis of liquid interfaces,

however, is complicated by their inherent roughness, i.e., the surface of a given fluid is corrugated by thermal fluctuations, or capillary waves [4,5]. This means that when the average profile of a given property is computed based on a fixed reference frame (we will call this the "global" profile), it will be smoothed by the instantaneous fluctuations of the position of the interface itself. So, contrary to the case of solid-fluid systems, in fluid-fluid interfaces one must develop a procedure to decouple the capillary wave corrugations from the averaging procedure in order to reveal the underlying structure of each phase (thus obtaining an "intrinsic" profile).

The most obvious property to examine when studying interfacial systems is density. The global density profile is based on the average cross-section of the system, according to:

$$\rho_G(z) = \left\langle \frac{1}{A_0} \sum_{i=1}^{N} \delta\left(z - z_i\right) \right\rangle, \tag{1}$$

where N is the number of molecules, z_i is their coordinate along the axis perpendicular to the interface, and A_0 is the nominal cross-sectional area. The intrinsic profile, on the other hand, is based on a local reference frame and is given by:

$$\rho_I(z) = \left\langle \frac{1}{A_0} \sum_{i=1}^{N} \delta\left(z - z_i + \xi\left(x_i, y_i\right)\right) \right\rangle, \tag{2}$$

where ξ is the instantaneous position of the surface, and x_i and y_i are the molecular coordinates in the plane parallel to the interface. It is immediately apparent from equation (2) that to compute the intrinsic profile one must determine the instantaneous position of the interface at each cross-sectional point. Although an alternative procedure has recently been proposed [6], in the majority of methods designed to compute intrinsic profiles [7-11] ξ is calculated by first identifying a set of sites that belong to the interfacial layer and then approximating the surface by a (continuous or discrete) function running through the centers of those sites.

In a previous paper [12], we have compared in detail the available methods for determining the true set of interfacial molecules for a liquid-liquid interface, using the water/CCl_4 interface as a prototype system. Four algorithms were tested: i) the Intrinsic Sampling Method (ISM) [8,13-17]; ii) the Grid-Based Intrinsic Profile (GIP) method [9,18]; iii) the Identification of Truly Interfacial Molecules (ITIM) procedure [19,20]; and iv) the Surface Layer Identification (SLI) method [11]. We have demonstrated that in order to obtain a realistic description of the surface layers, each method requires an adjustable control parameter, and this led to the development of an improved version of the SLI protocol (which we have called SLIx) [12]. Consistent results between different methods were obtained using the optimal values of the respective control parameters. The ISM provided a very accurate and self-consistent description of the surface, but at the cost of a much larger computational effort, which may prevent its application in more complex systems. Conversely, the GIP method was by far the fastest algorithm of all but showed some limitations that jeopardize its accuracy in identifying the true set of interfacial molecules. The ITIM emerged as the method of choice for routine detections of the intrinsic surface sites, combining good accuracy with a fast computational procedure that can be applied to both liquid-liquid and liquid-vapor interfaces.

Once the positions of all the interfacial molecules have been determined, the next step for computing the intrinsic profile is to define a mathematical function $\xi(x,y)$ for all possible values of x and y. In other words, given the value of ξ at a certain set of points (the positions of the interfacial molecules), one must find a way to estimate it at other points on the (x,y) plane. Naturally, many alternative ways to achieve this may be devised [8-11]. In the present paper, we critically compare several methods for calculating intrinsic profiles given a certain surface site distribution and assess whether or not these methods yield intrinsic profiles that are consistent with each other. Our analysis has led to the improvement of some of these methods, and to the development of a new method for calculating intrinsic profiles that yields accurate results with minimal computational effort. It is important to emphasize, however, that alternative procedures exist for computing intrinsic density profiles which do not require the definition of a set of surface sites [6], but these are outside the scope of the present study. The paper is organized as

follows: in the next section we present details of our molecular dynamics (MD) simulations of the water/carbon tetrachloride interface; in sections 3.1 to 3.5 we describe and present results for the different methods studied, which are then compared in section 3.6; finally, our main conclusions are summarized in section 4.

2. Simulation Details

Molecular dynamics simulations of the water/CCl_4 liquid-liquid interface were carried out using the GROMACS simulation package [21] on the canonical (N,V,T) ensemble. The system was composed of 4000 water and 2000 CCl_4 molecules, and was started from a configuration generated in a previous study [20]. The dimensions of the simulation box in the x, y and z directions were, respectively, 5.0, 5.0 and 17.9 nm, and periodic boundary conditions were applied in all Cartesian directions. The temperature of the system was kept constant at 298 K by means of the Berendsen thermostat [22]. Water molecules were described by the rigid, four-site TIP4P model [23], with the geometry constrained using the SETTLE [24] algorithm. Carbon tetrachloride was described by the rigid five-site model of McDonald et al. [25], with the geometry held fixed by applying the SHAKE [26] algorithm. Thus, the total potential energy of the system was calculated as the sum of all pairwise interaction energies, including both Lennard-Jones and Coulomb electrostatic terms. All interactions were truncated to zero beyond the molecule center-based cut-off distance of 14.0 Å, with the long range-part of the Coulomb interactions accounted for using the Particle Mesh Ewald (PME) method [27]. The equations of motion were integrated in time steps of 2 fs, and the system was equilibrated for a period of 1 ns. Subsequently, 2000 sample configurations separated from each other by 0.5 ps were saved for the analyses, and all results were averaged over these configurations. In order to avoid possible drifts, the sampled configurations were translated along the interface normal axis z in such a way that the position of the center-of-mass of the organic phase was moved to the origin of the coordinate axes.

3. Results and Discussion

In order to compare the different methods for approximating $\xi(x,y)$, given a certain set of surface site positions, one must apply them to the same surface site distribution. Therefore, except where explicitly noted, all density profiles were computed based on surface site distributions for both components determined using the ITIM procedure [19,20], with probe sphere radii (R_P) of 0.125 nm for water and 0.2 nm for CCl_4. These radii were previously shown to yield the optimal description of each of those surfaces, yielding dimensionless surface layer densities (defined as $n_S = N_S\sigma^2 / L_x^{\,2}$, where N_S is the number of surface molecules, σ is a characteristic site diameter, and L_x is the simulation box length in the directions parallel to the interfacial plane) of 1.13 for water and 0.65 for CCl_4 [12]. Two types of density profiles were compared for each method: i) "opposing" profiles, i.e., water density relative to the position of the organic interface (ρ_{WO}) and CCl_4 density relative to the water interface (ρ_{OW}); ii) "self" profiles, i.e., water density relative to the position of the water interface (ρ_{WW}) and CCl_4 density relative to the CCl_4 interface (ρ_{OO}). For all profiles, the origin is located at the center of the simulation box. In all cases, we discuss density profiles for the leftmost interface of the system, but the results are equivalent when the rightmost interface is considered. In the following sections, we describe each method in detail and analyze the resulting density profiles. Figure 1 shows a schematic representation of each of the methods studied.

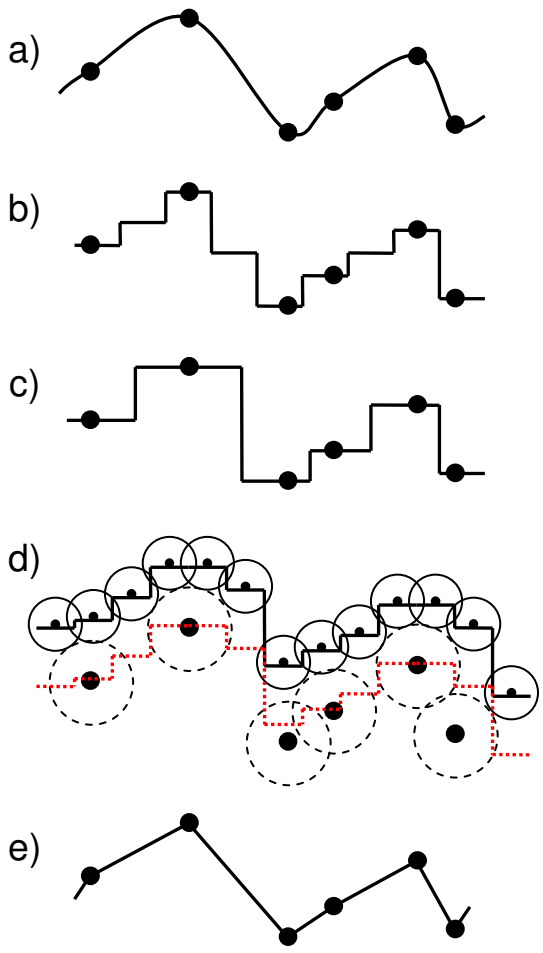

Figure 1 – Schematic one-dimensional representation of each of the methods used to calculate intrinsic profiles based on the same set of surface site positions. The surface sites are represented by black circles and the full line represents the corresponding approximation to the function $\xi(x,y)$ for: a) Fourier function; b) modified GIP method; c) Voronoi tessellation; d) covering surface; e) triangular interpolation. In panel d, the dashed circles represent the exclusion spheres of the surface sites, the small open circles are the probe spheres used in the ITIM method, and the red dotted line is the surface function shifted downward by a constant value (see Section 3.4 for details).

3.1 The Fourier function method

Perhaps the most natural method for approximating $\xi(x,y)$ is to fit an analytical function that passes through the positions of all surface sites (see Figure 1a). This is the idea behind the

ISM method, originally developed by Chacón and Tarazona [8]. The intrinsic interface is defined as the minimal area surface that goes through all the atomic sites located at the interface. A smooth mathematical function passing through the coordinates of the surface sites, $(\mathbf{R}_i, z_i) = (x_i, y_i, z_i)$, is constructed in terms of a sum of Fourier components:

$$\xi(\mathbf{R}, q_m) = \sum_{0 \le |\mathbf{q}| \le q_m} \hat{\xi}_q e^{i\mathbf{q}\cdot\mathbf{R}} = \sum_{\mu^2+\nu^2 \le {n_M}^2} a_{\mu\nu} f_\mu(x) f_\nu(y), \quad (3)$$

where **q** is the wavevector, with maximum wavevector cutoff q_m. The second expression is a more useful representation in terms of sines and cosines, with $f_0(x) = 0$, $f_\mu(x) = \cos(2\pi\mu x/L_x)$, and $f_{-\mu}(x) = \sin(2\pi\mu x/L_x)$ for integer values of μ>0, where $a_{\mu\nu}$ are real coefficients with indices running from $-n_M$ to n_M. The value of n_M is set to $\approx L_x/\sigma$, such that all possible wavevectors down to atomic resolution are used. As characteristic site diameters, we take the Lennard-Jones diameters of the water oxygen and of the CCl_4 carbon. The intrinsic surface is obtained, subject to the minimal area requirement, by minimizing the function [16]:

$$W = \frac{1}{2}\sum_{i=1}^{N_S}\left(z_i - \xi(\mathbf{R}_i)\right)^2 + \frac{\phi {L_x}^2}{2}\sum_{|\mathbf{q}| \le q_m} q^2 \left|\hat{\xi}_q\right|^2, \quad (4)$$

where N_S is the total number of surface sites, and ϕ is a parameter that sets a maximum threshold distance between the surface function and the coordinates of the surface sites (we use $\phi = 10^{-8}$ as suggested by the authors [16]). Combining equations (3) and (4), we obtain a set of linear equations with respect to the coefficients $a_{\mu\nu}$:

$$\sum_{\mu'\nu'}\left[\sum_{i=1}^{N_S} f_{\mu'}(x_i) f_{\nu'}(y_i) f_\mu(x_i) f_\nu(y_i)\right] a_{\mu'\nu'} + 4\pi^2\delta(\mu^2+\nu^2) a_{\mu\nu} = \sum_{i=1}^{N_S} z_i f_\mu(x_i) f_\nu(y_i) \quad (5)$$

The above equations were solved for the coefficients $a_{\mu\nu}$ by an efficient LU decomposition algorithm [28].

In Figure 2 we plot the intrinsic number density profiles (both opposing and self profiles) obtained by fitting a Fourier function to the ITIM surface site positions for both water and CCl_4. In this figure and henceforth when plotting the self profiles, we omit for the sake of clarity the extremely narrow peak corresponding to the first interfacial molecular layer of each phase. Also shown are the global profiles (dashed lines), i.e., the density profiles averaged using a fixed reference frame, and the interfacial site distributions obtained with the ITIM method (dashed-dotted lines). The global profiles show the usual smoothing due to the capillary wave fluctuations of the interface – the organic profile shows only very small evidence of layering, while the water profile rises monotonically from zero to the bulk value, with no layering observed. The intrinsic profiles, on the contrary, reveal the underlying structure of the interfaces in the form of pronounced layering effects.

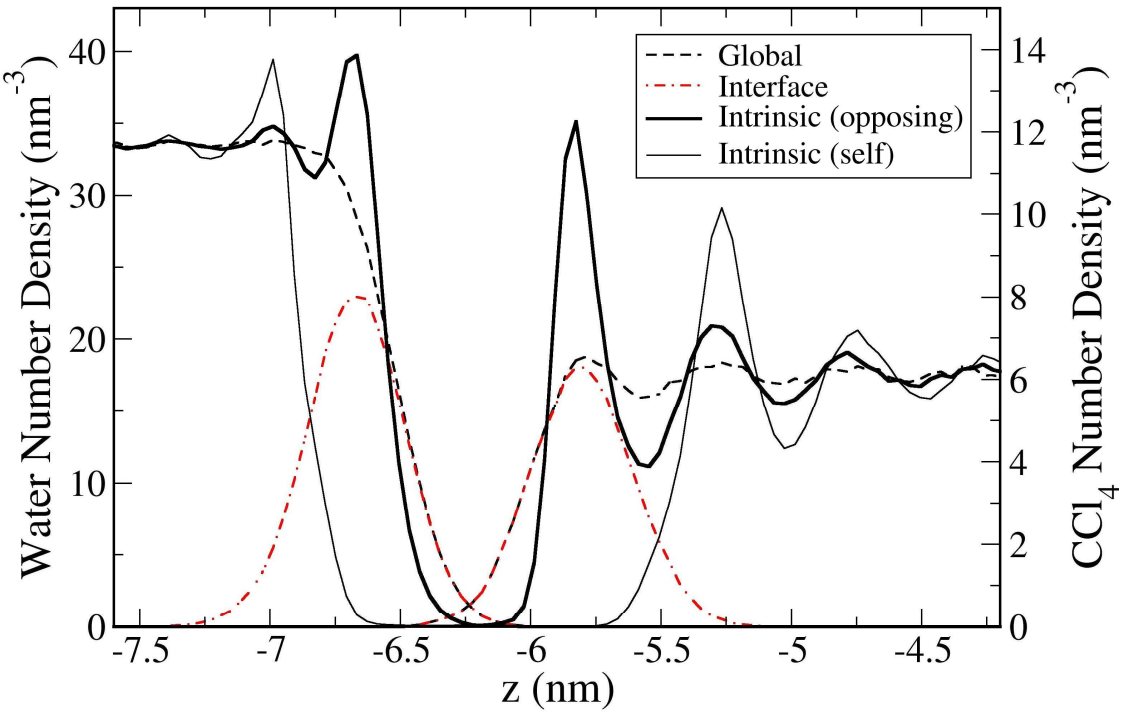

Figure 2 – Density profiles for water (left curves and left axis) and CCl_4 (right curves and right axis). The distributions of interfacial molecules (red dashed-dotted lines) were obtained from the ITIM method with optimal values of R_P. Intrinsic profiles (full lines) were calculated by fitting a Fourier function through the positions of the interfacial sites for each phase. The curves for CCl_4 are shifted by 0.4 nm to the right for clarity.

It is clear from Figure 2 that this layering is much more dramatic for CCl_4 than for water. The ρ_{WO} profile shows a large first peak that corresponds to the interfacial water layer, followed by a much smaller peak for the second molecular layer beneath the interface. In the ρ_{WW} profile, the interfacial layer assumes the form of a very narrow peak (not shown), while the peak for the second layer becomes more pronounced. In this profile, one can only barely distinguish a small hump corresponding to a third molecular layer beneath the interface. This means that beyond the second molecular layer, water molecules are essentially showing a bulk-like structure. The ρ_{OW} profile, on the other hand, exhibits at least three pronounced peaks. The peaks corresponding to the second and third layers beneath the CCl_4 interface are enhanced in the ρ_{OO} profile, and evidence of a fourth layer can even be discerned close to the right edge of the plot. This different behavior of the water and organic phases has been observed previously for other liquid-liquid interfaces [9,18]. In the remainder of this paper, the intrinsic profiles shown in Figure 2 will be used as a reference for comparison with other calculation methods.

Before we move on, however, it is useful to analyze the effect of different interfacial site distributions on the resulting intrinsic profiles. In Figure 3 we compare the opposing density profiles calculated by fitting Fourier functions to the surface site distributions obtained from the ITIM and from the ISM methods (see our previous paper [12] for details of the calculation procedures). In other words, we are using the same method to compute the profiles, but we are starting from two (slightly) different underlying sets of surface sites. As we can see from the figure, there is a very good agreement between the two sets of profiles, particularly for water, where the profiles match almost perfectly. The organic profile obtained from the ISM

distribution is slightly shifted to the right (by about 0.035 nm), relative to the one obtained from the ITIM distribution, and shows a small tail extending into the water phase. These small differences are likely due to the somewhat different procedures used to find the set of interfacial molecules, as discussed in detail in our previous paper [12], and are not deemed significant for our subsequent analysis.

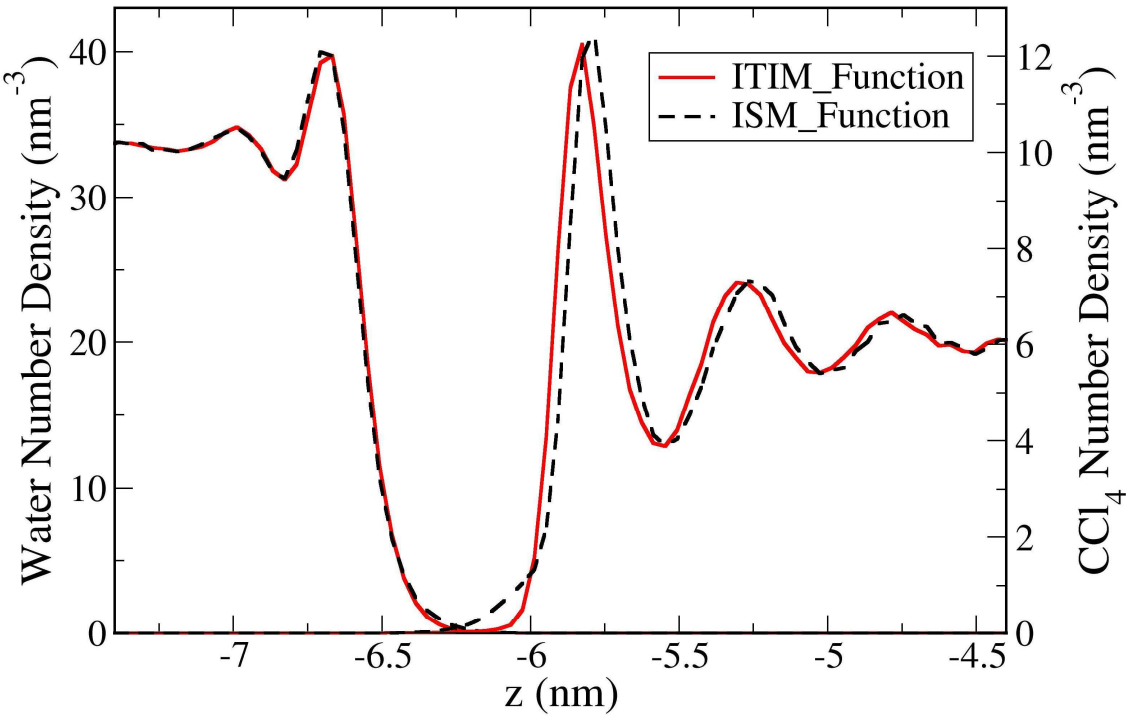

Figure 3 – Opposing intrinsic density profiles for water (left curves and left axis) and CCl_4 (right curves and right axis) obtained by fitting a Fourier function to surface site distributions obtained from the ITIM (full red lines) and the ISM (dashed black lines) methods. The curves for CCl_4 are shifted by 0.4 nm to the right for clarity.

3.2 The Grid-based Intrinsic Profile method

The next method we analyze is based on discretizing the surface of each phase using a regular square lattice. It is perhaps on the opposite end of the spectrum from the Fourier function method, in the sense that it is expected to be somewhat less accurate, but much faster than the latter [12]. In the original GIP method [9,18], the plane parallel to the interface was

divided into a grid of $N_G \times N_G$ squares. The optimum grid resolution was found to be approximately given by $N_G \approx L_x/\sigma$, where σ was the diameter of the largest atomic site in each liquid [9,18]. In each of the resulting rectangular prisms of transverse size L_x/N_G, the atomic center closest to the opposite phase was found, and its z position was used as an estimate of $\xi(x,y)$ for all other points located inside that prism. Intrinsic profiles were then straightforwardly computed from this discretized surface by applying equation (2).

Our first, somewhat naïve, approach was to directly apply the original GIP method to the interfacial layer determined with the ITIM method, but unfortunately this led to a complete failure. The reason is that the original GIP method is based on a one-to-one correspondence between each center of an interfacial molecule and each prism of the grid. When applied directly to the ITIM list of surface sites, and depending on the resolution, a given prism may contain more than one surface site center or may not contain any surface sites at all. At low resolutions (small values of N_G), the first situation is much more common than the second, which leads to a definition of the interface that is too coarse. As the resolution is increased, the first situation practically disappears, but the second one becomes more common – at high resolutions, several of the prisms include no molecular centers at all, and the value of $\xi(x,y)$ in those prisms becomes undefined. Needless to say, the calculated profiles for all but the lowest grid resolutions are virtually meaningless.

A possible solution to circumvent this problem is to carry out two passes over the list of surface sites. In the first pass, the original GIP method is applied and values of $\xi(x,y)$ are attributed to the grid points that contain interfacial molecules. In the second pass, the value of $\xi(x,y)$ at the remaining grid points is interpolated from values at neighboring points determined in the first pass. More precisely, a weighted interpolation is performed using the following scheme: i) in each direction, the nearest grid point that has an attributed value of $\xi(x,y)$ is found; ii) the number of grid points (n) that separate the central point from each of its four neighbors is counted; iii) the value of $\xi(x,y)$ for the central point is calculated from:

$$\xi(x,y) = \frac{\sum_{i=1}^{4} \frac{\xi_i}{n_i}}{\sum_{i=1}^{4} \frac{1}{n_i}}, \quad (6)$$

where the summations are performed over all four directions of the square lattice (positive x, negative x, positive y, and negative y). A schematic representation of the surface obtained using this method is depicted in Figure 1b. In this diagram, six of the grid points contain centers of interfacial sites (ξ is determined in the first pass), while three of them do not (ξ is determined by interpolation in the second pass).

The resulting profiles obtained with the modified grid method are shown in Figure 4 for increasing values of the grid resolution. The performance of the method is a trade-off between two effects – at low resolution, the grid is simply too coarse to provide an accurate description of the surface, while if the resolution is too high, the number of values of $\xi(x,y)$ that are not defined in the first pass is too large and the error of the interpolation procedure becomes pronounced. As a consequence, an optimal grid resolution, providing the best possible description of the surface, can be determined. For this system, the optimal values of N_G are 14 for the CCl_4 surface and 40 for the water surface (thick black lines in Figure 4), calibrated to provide the best possible agreement with the profiles obtained from the Fourier function method. As we can see, using these values the method yields a very good approximation of both the opposing and self profiles.

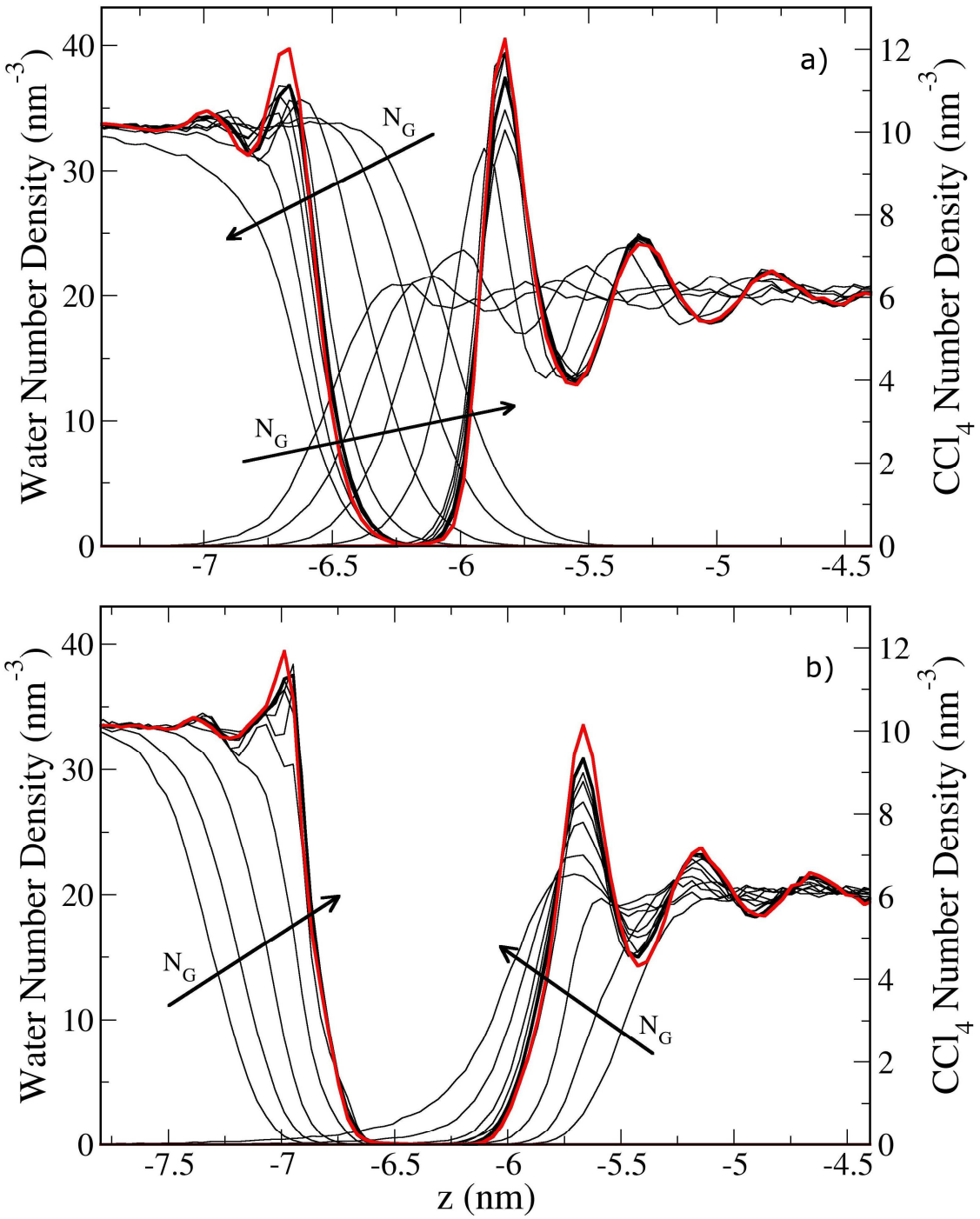

Figure 4 – Opposing (a) and self (b) intrinsic density profiles for water (left curves and left axis) and CCl_4 (right curves and right axis) obtained by applying the modified grid method with increasing values of N_G – 1, 2, 4, 8, 14, 20, 30, 40, 60, and 80 (directions of increasing N_G are shown by arrows). The thick black lines are profiles corresponding to the optimal resolution (see text). Also shown are the corresponding profiles calculated from the Fourier function

method (thick red lines). In panel a), the curves for CCl_4 are shifted by 0.4 nm to the right for clarity.

3.3 The Voronoi tessellation method

As we have seen in the previous section, a straightforward application of the original GIP method to the set of interfacial molecules failed because some grid squares did not contain any atomic centers, and this led us to propose the modifications described above. However, a different approach is possible that avoids this problem altogether – applying a Voronoi tessellation to the surface layer. The Voronoi tessellation method was, to our knowledge, first applied by Pandit et al. [10] to water/lipid bilayer interfaces, where the interfacial sites were considered to be the phosphorous atoms of the lipid molecule. It was later adapted by Chowdhary and Ladanyi [11] to several water/hydrocarbon interfaces, as part of their SLI method for identifying surface sites and computing intrinsic profiles.

In short, the algorithm proceeds as follows: i) the coordinates of all the surface sites are projected onto the (x,y) plane; ii) this plane is then divided into a set of Voronoi polygons (or Voronoi simplices), each of which defines the region of the plane that is closest to each of the surface sites; iii) the value of $\xi(x,y)$ at all points that fall inside a given Voronoi simplex is approximated by the z coordinate of the site located at the center of that simplex. A schematic diagram of this method is shown in Figure 1c. Because there is a one-to-one correspondence between each surface site and each Voronoi polygon, $\xi(x,y)$ is defined in the entire plane, and the problem observed above for the GIP method disappears.

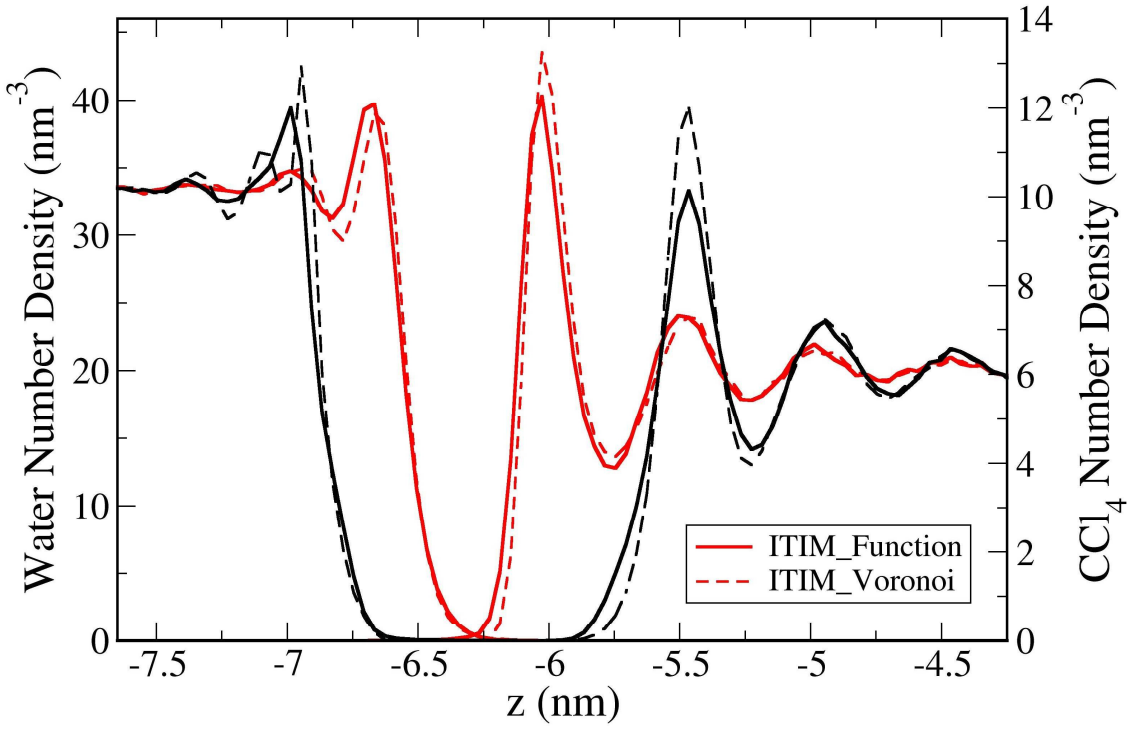

Figure 5 – Opposing (red lines) and self (black lines) intrinsic density profiles for water (left curves and left axis) and CCl_4 (right curves and right axis). Solid lines are profiles obtained with the Fourier function method, while dashed lines are profiles obtained with the Voronoi tessellation method. The curves for CCl_4 are shifted by 0.2 nm to the right for clarity.

In Figure 5, we compare the intrinsic density profiles calculated with the Voronoi method to those obtained in the reference case (i.e., using a continuous Fourier function to approximate the surface). The Voronoi method yields a good estimate of the opposing profiles, but is not so successful in describing the self profiles. For the ρ_{WW} profile, in particular, an unphysical double peak appears in the second molecular layer beneath the surface, which is most likely an artifact induced by the discrete approximation of the surface function $\xi(x,y)$.

3.4 The "covering surface" method

Our previous comparison of methods to identify the true set of interfacial molecules [12] has shown that the ITIM method yields an accurate description of the surface layers with minimal computational effort. However, one of the drawbacks of this method is that it does not

provide a prescription to calculate intrinsic profiles once the surface sites are identified. In this section, we explore the possibility of taking advantage of the construction of the ITIM procedure [19,20] to develop a method for computing intrinsic density profiles. We have named this the "covering surface" method, for reasons that will become apparent soon.

In the ITIM method, a grid of test lines that run perpendicularly to the interface is constructed, and a probe sphere of radius R_P is run along each of the test lines. The probe is stopped as soon as it collides with one of the atomic sites of the phase it is probing, and that site is labeled as interfacial. With an appropriate choice of R_P [12], one is able to obtain a list of Cartesian coordinates of all surface sites, as well as a list of positions of the probe spheres after they are stopped. Both these sets of points are shown in the diagram of Figure 1d.

In all the previous sections, we have used the coordinates of the actual surface sites as a basis to compute the intrinsic density profiles. A major difficulty associated with this approach is that the coordinates of the surface sites do not lie on a regular grid, which makes it harder to approximate $\xi(x,y)$ using a discrete function (see, e.g., the discussion in section 3.2). However, the coordinates of the probe spheres *do* lie on a regular grid. The idea behind the covering surface method is to take advantage of this and use the set of probe sphere positions as a basis for the calculation of the intrinsic profiles (see Figure 1d) instead of the positions of the actual surface sites. The value of $\xi(x,y)$ for each square of the grid is taken as the z coordinate of the stopped probe sphere corresponding to that position of the grid. Calculation of the profiles using this procedure then becomes as efficient as in the original GIP method – it is simply a matter of finding which molecules lie inside each square of the grid. The drawback, of course, is that we are no longer calculating the profile relative to the center of the surface sites, but to the center of a surface obtained by covering the surface sites with a layer of regularly arranged overlapping spheres – hence the name "covering surface".

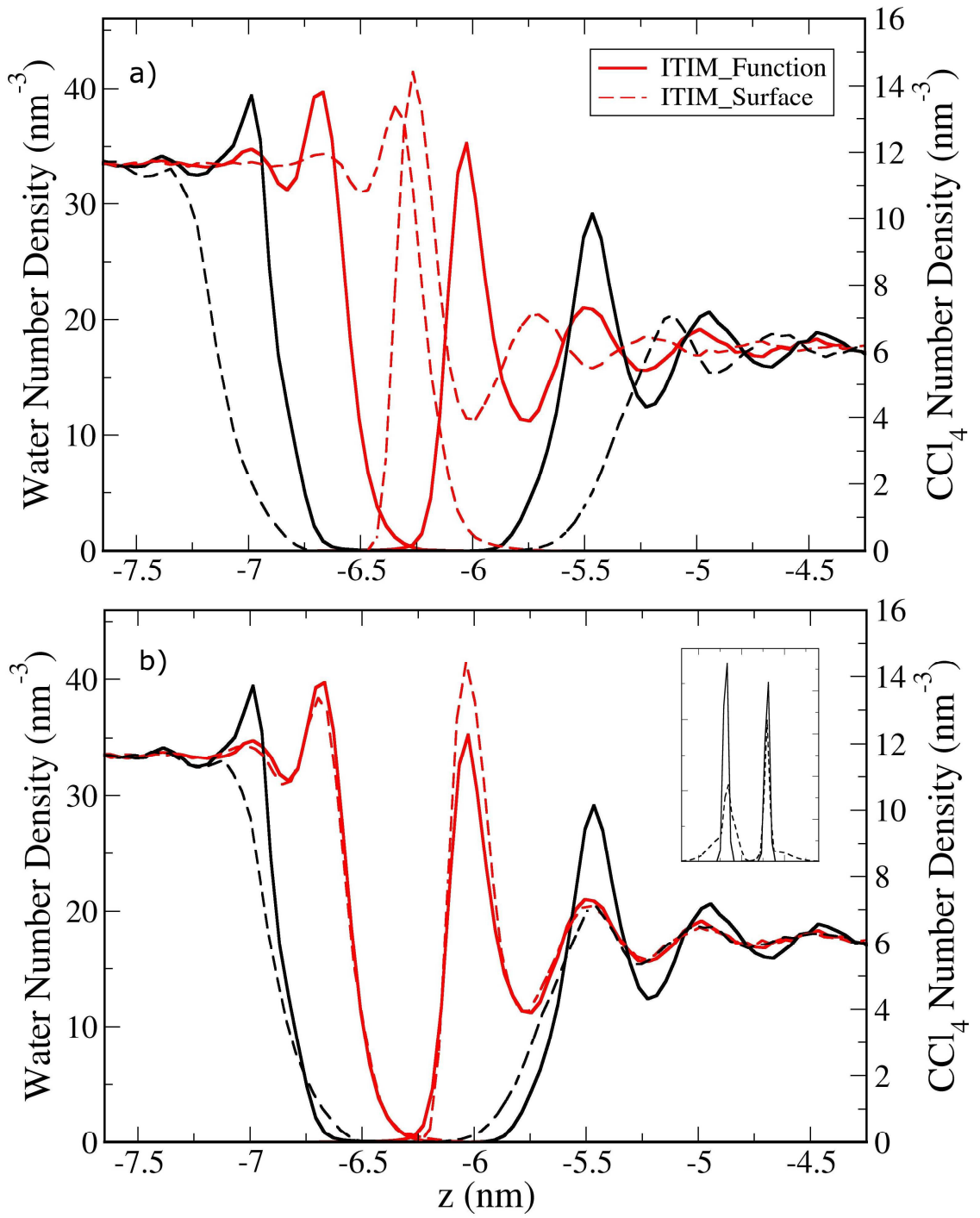

Figure 6 – Opposing (red lines) and self (black lines) intrinsic density profiles for water (left curves and left axis) and CCl_4 (right curves and right axis). Solid lines are profiles obtained with the Fourier function method, while dashed lines are profiles obtained with the covering surface method. The curves for CCl_4 are shifted by 0.2 nm to the right for clarity. In panel b), the profiles obtained with the covering surface method are additionally shifted along the *z*

coordinate to yield the best possible agreement with the reference profiles (see text for details). The inset shows the self profiles of the interfacial site distributions obtained with both methods.

Results obtained using this method are shown in Figure 6a. It is immediately apparent that the profiles are displaced along the z direction, relative to the profiles obtained with the Fourier function method. This is to be expected, because we are now calculating the profiles using a reference surface that does not go through the surface sites themselves (see full black line in Figure 1d). More precisely, profiles calculated relative to the CCl_4 surface (ρ_{WO} and ρ_{OO}) are displaced to the right (positive z) because the reference surface moves to the left, and vice-versa for profiles relative to the water surface (ρ_{OW} and ρ_{WW}). A possible way to correct this effect is to shift back the function $\xi(x,y)$ in the z direction by a constant value δ (see red dotted line in Figure 1d) so that it passes close to the centers of the surface sites. If we assume that every probe sphere hits a surface site at an angle of 180º (i.e., that each grid line passes through the center of a surface site), then the value of δ will be precisely the sum of R_P and the collision radius of the surface site. In reality, however, the probe spheres will hit the surface sites at angles that range between 180 and 90º, which means that δ will be somewhat lower than that "ideal" value. We have adjusted the value of δ for each surface so that the position of the first peaks of the ρ_{WO} and ρ_{OW} profiles obtained with the covering surface method matched those of the corresponding profiles calculated with the Fourier function. The optimal values were δ_O = -0.35 nm and δ_W = +0.23 nm. For both phases, this turns out to be precisely 82% of the maximum value described above (i.e., the sum of R_P and the collision radius of the surface site). The agreement may be fortuitous, but nevertheless lends further consistency to the ITIM method.

The intrinsic profiles shifted by the above values of δ are plotted in Figure 6b. There is very good agreement with the Fourier function results for opposing profiles (particularly for the ρ_{WO} profile), but poor agreement for the self profiles. This can be understood by thinking about the construction of the covering surface. Because we are using a probe sphere with a finite

radius, the covering surface will necessarily be smoother than the actual surface going through the centers of the surface sites. In other words, we are only partially removing the thermal fluctuations of the interface position. As a consequence, even if we shift back the covering surface, several of the surface sites will be located at a certain distance from the surface, mostly on the bulk side (notice, for example, the third and sixth surface sites counting from left to right in the diagram of Figure 1d). Therefore, the first peak of the self profiles, corresponding to the density of the interfacial layer relative to itself, is no longer a well-defined narrow peak, but instead shows long tails on both sides (see inset in Figure 6b). This causes an artificial smoothing of the intrinsic profiles, which is particularly noticeable in the self profiles. The main conclusion of this analysis is that intrinsic profiles should be calculated relative to a surface function that passes as close as possible to the centers of the surface sites themselves, thus completely removing all thermal fluctuations of the interface. Because it does not satisfy this requirement, the covering surface method is inadequate for the calculation of intrinsic profiles.

3.5 The triangular interpolation method

The last method we consider is an entirely new approach for constructing a mathematical surface $\xi(x,y)$ that runs through the centers of all the surface sites, based on the idea of triangular interpolation on a plane. Triangular interpolation is the equivalent of linear interpolation extended to bivariate functions (see diagram of Figure 1e). To compute the value of ξ at a given point I in the (x,y) plane, the algorithm works as follows:

1. Project the coordinates of all the surface sites onto the (x,y) plane;
2. Sort the surface sites by increasing distance of their (x,y) projections to point I;
3. Build a triangle connecting the three surface sites whose projections lie closest to point I, i.e., the first three sites on the above list (we shall call these A, B and C, in order of proximity to I);
4. Check if point I is enclosed by the triangle thus formed. This is verified if the following condition is met:

$$A_{ABC} = A_{ABI} + A_{AIC} + A_{IBC}, \quad (7)$$

where A_{IJK} is the area of the triangle formed by points I, J and K;

5. If equation (7) is not met, go back to step 3, but replace point C by the fourth closest surface site to I, and so on, until condition (7) is met;

6. Apply the triangular interpolation formula, equation (8), to estimate $\xi(x,y)$ at point I:

$$\xi_I = z_A \frac{(x_B - x_I)(y_C - y_B) - (y_B - y_I)(x_C - x_B)}{(x_B - x_A)(y_C - y_B) - (y_B - y_A)(x_C - x_B)} + z_B \frac{(x_C - x_I)(y_A - y_C) - (y_C - y_I)(x_A - x_C)}{(x_B - x_A)(y_C - y_B) - (y_B - y_A)(x_C - x_B)} + z_C \frac{(x_A - x_I)(y_B - y_A) - (y_A - y_I)(x_B - x_A)}{(x_B - x_A)(y_C - y_B) - (y_B - y_A)(x_C - x_B)} \quad (8)$$

where x_J, y_J, and z_J are the Cartesian coordinates of point J.

In a small percentage of cases, condition (7) is not satisfied even after looping over the entire list of surface sites built in step 2. This happens, for example, when the angle ∠AIB is very close to zero (in such a case it is very difficult to find a third point that satisfies equation (7)). In such cases, we simply take $\xi(x,y) = z_A$ at that point I. This simplification was only necessary in about 1% of the cases. We are currently working on a more elegant way to deal with these extreme cases, but for the time being this simplified approach has been found to be quite effective.

In Figure 7 we compare the results obtained using the triangular interpolation method with the intrinsic profiles calculated with the Fourier function. It is clear that the interpolation method provides an excellent approximation of all profiles. With this method, we are essentially performing a local approximation of the underlying surface in the vicinity of a given point by a tilted plane. As we will see in the next section, this turns out to yield very accurate profiles at a fraction of the computational cost of fitting a Fourier function that passes through all of the surface sites.

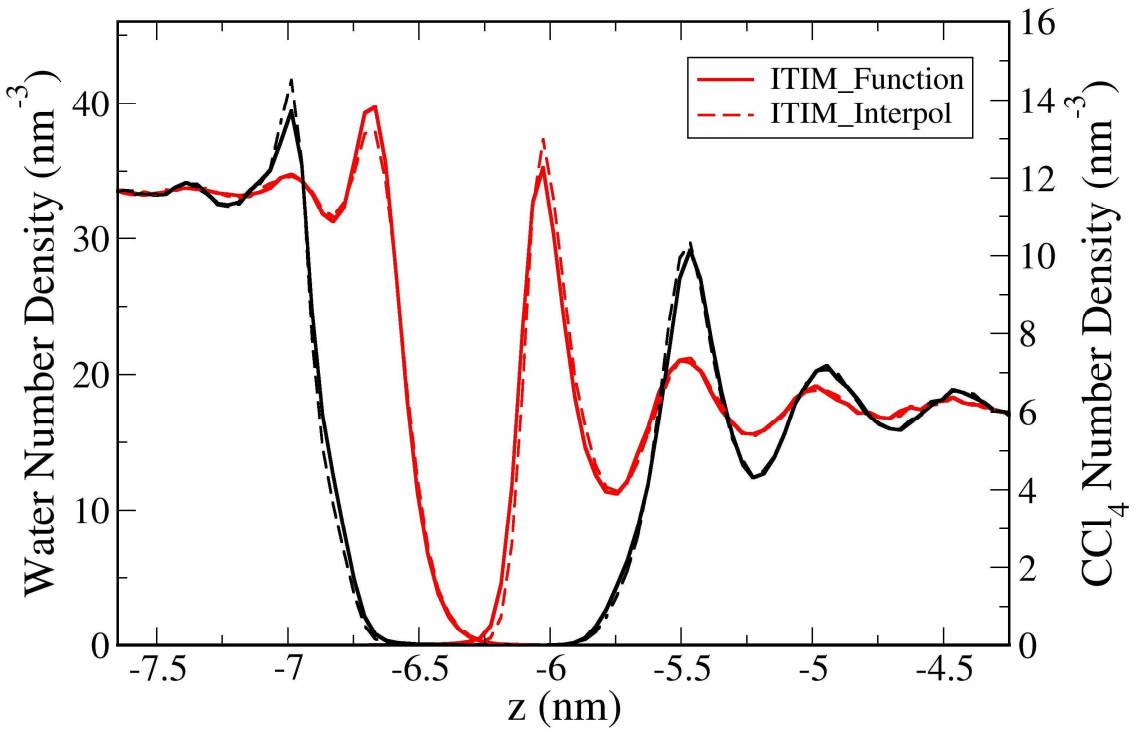

Figure 7 – Opposing (red lines) and self (black lines) intrinsic density profiles for water (left curves and left axis) and CCl_4 (right curves and right axis). Solid lines are profiles obtained with the Fourier function method, while dashed lines are profiles obtained with the triangular interpolation method. The curves for CCl_4 are shifted by 0.2 nm to the right for clarity.

3.6 Comparison between all methods.

In this final section, we compare all the methods described above in terms of their accuracy and speed of computation. Figure 8 shows all the intrinsic profiles obtained with the five different methods. In qualitative terms, all methods provide reasonable estimates of the opposing profiles (Figure 8a), with the Voronoi tessellation faring slightly worse than the rest for the ρ_{WO} profile (the first peak is somewhat distorted) and the covering surface method yielding the worst results for the ρ_{OW} profile (the first peak is too high). The differences between the methods become more evident when we look at the self profiles (Figure 8b). In this case, only the modified GIP method and the triangular interpolation are capable of capturing the correct qualitative shape of the profiles. The Voronoi method generates profiles with excessive structure, particularly for the ρ_{WW} profile where the first peak becomes split into two, while the

covering surface method produces profiles that are far too smooth (the first peak of the ρ_{WW} profile practically disappears). Overall, the best qualitative results are obtained with the triangular interpolation.

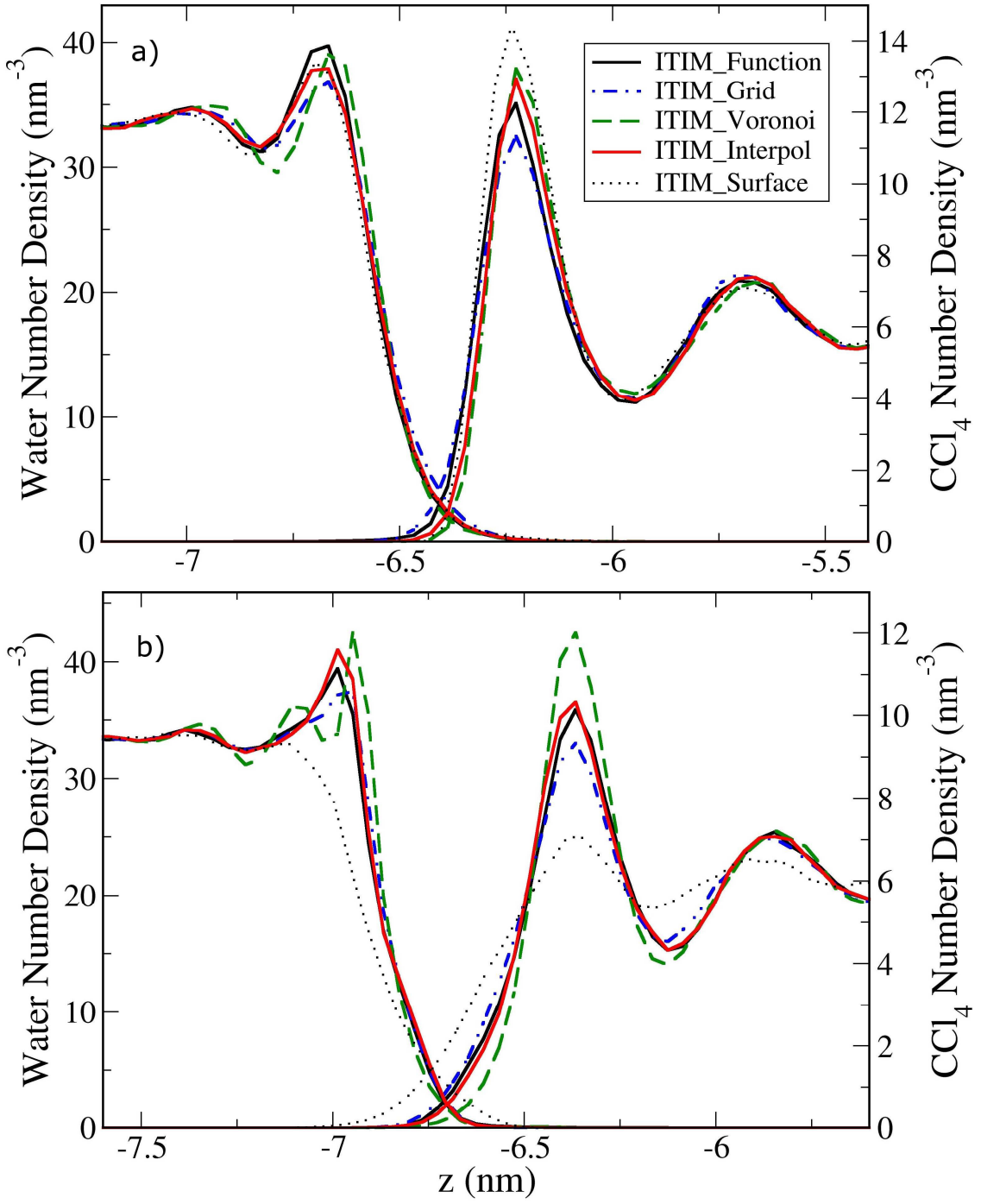

Figure 8 – Opposing (a) and self (b) intrinsic density profiles for water (left curves and left axis) and CCl_4 (right curves and right axis) obtained by applying all the different methods

considered in this paper. In panel b), the curves for CCl_4 are shifted by 0.7 nm to the left for clarity.

We have tried to quantify the precision of each method by computing the root mean square error of each profile relative to the corresponding reference profile (obtained with the Fourier function). For each method, the total relative error (ε_{JK}) for the intrinsic density profile of phase *J* relative to the surface of phase *K* was calculated from:

$$\varepsilon_{JK} = \frac{\sqrt{\sum_i \left(\rho_{JK,i}^{\mathrm{Ref}} - \rho_{JK,i}\right)^2}}{\rho_J^{\mathrm{Bulk}}}, \qquad (9)$$

where the superscript *Ref* refers to the reference density profile and the superscript *Bulk* refers to the average bulk density of the phase. The summation is carried out over all the bins used in the calculation of the density profiles. The estimated errors for the different methods are shown in Table 1. In agreement with our qualitative analysis, the best performance was achieved with the triangular interpolation, followed closely by the modified GIP method. The covering surface method suffers from the largest errors, particularly for the self profiles.

Table 1 – Comparison of the precision and computational efficiency of the different methods for calculating intrinsic profiles.

Method	ε_{WO}	ε_{OW}	ε_{WW}	ε_{OO}	Time[a] (s)
Function	--	--	--	--	68.37
GIP	0.0392	0.0633	0.0324	0.0667	0.768
Voronoi	0.0505	0.1433	0.0927	0.1333	0.777
Surface	0.0264	0.1522	0.1361	0.2200	0.759
Interpolation	0.0205	0.0987	0.0239	0.0456	1.316

[a] – Time taken to calculate all four intrinsic profiles in a single configuration.

Also shown in Table 1 are the computational times spent on calculating the intrinsic profiles for a single molecular configuration. As expected, the Fourier function method is slower than all the other methods by almost two orders of magnitude, which is due to the demanding process of solving equation (5) to obtain the Fourier coefficients. In our previous paper [12], this was shown to be the main reason for the slow performance of the ISM method relative to the other algorithms for identifying the true set of surface sites. Therefore, although approximating $\xi(x,y)$ by a continuous analytical function that passes through all surface sites is the most accurate and physically realistic approach [8,13], the excessive computational requirements mean that its routine application in the intrinsic analysis of fluid interfaces should be quite difficult. The other four methods considered here show very similar performances in terms of computer time, with the triangular interpolation being slightly slower than the other three (by a factor of about 1.7). However, the excellent performance of this method in reproducing the intrinsic density profiles, both qualitatively and quantitatively, more than make up for the slightly larger computational requirements. The modified GIP method is also a good possibility, but has the disadvantage of requiring the tuning of the grid resolution.

4. Conclusions

In this paper, we have concluded our detailed comparison of methods to perform intrinsic analyses of fluid interfaces, by focusing on procedures to calculate intrinsic density profiles from knowledge of a surface site distribution. Two of the methods studied – the Fourier function [8] and the Voronoi tessellation [10,11] – were previously developed by other authors, two other methods – the covering surface and the triangular interpolation – are newly proposed algorithms, and one of them – the modified GIP method – is an improvement over an existing procedure [9]. One conclusion of our study is that the reference surface from which intrinsic profiles are calculated should pass as close as possible through the actual positions of the surface sites. Therefore, the covering surface method, which is based on constructing a reference surface from the positions of a regular array of probe spheres that are in contact with

all surface sites, was found to yield inaccurate results, particularly for the self profiles. Both the Voronoi tessellation and the GIP method are based on a discrete representation of the reference surface in terms of a collection of horizontal polygons – in the former they are the Voronoi simplices, while in the latter they are squares of uniform size. The Voronoi tessellation has the advantage of providing a simple and unambiguous method to define the surface at every point of the (x,y) plane. Unfortunately, the discretization level seems to be too coarse, which causes the intrinsic profiles to display some spurious structures. The GIP method required a modification to ensure that the surface function was properly defined at every point. This modified GIP method is extremely fast and yields good results when an optimal grid resolution is employed. The disadvantage is that this optimal resolution is not known *a priori* and depends on the nature of the phases being probed, making its application to a wide range of systems more difficult. The Fourier function method is a natural choice for the surface function, but suffers from large computational requirements. Of all the methods examined, the new triangular interpolation seems to be the ideal approach, since it combines excellent accuracy with speed of computation. The success of this method lies in describing the surface by a collection of tilted triangles, thus providing a very good local approximation of a continuous function at a fraction of the computational cost.

By taking our two papers together, we are in a position to propose the best combination of methods to perform intrinsic analyses of fluid interfaces. Based on our critical comparisons, we propose using first the ITIM method for identifying the true set of interfacial sites [12], followed by the triangular interpolation method to calculated intrinsic profiles. This combination provides an accurate description of the underlying structure of fluid interfaces with relatively low computational expense, and is generally applicable to both liquid-liquid and vapor-liquid interfaces involving complex molecular species. Although we have focused only on intrinsic density profiles, the approach is applicable in principle to intrinsic profiles of any other structural or dynamical property. Application of these methods to interfaces that are not flat (e.g., the surfaces of micellar aggregates) should require some modifications, but is also possible in principle. Future work will be devoted to this topic. We believe the present work

will contribute to a widespread application of intrinsic analysis methods to systems that involve fluid interfaces.

Acknowledgements. The authors would like to acknowledge Livia Bartok-Partay for helpful discussions during the preparation of this manuscript. This work was partly supported by the Hungarian OTKA Foundation under project No. 75328, and by the Hungarian-Portuguese Intergovernmental Science and Technology Program. P. J. is a Bolyai János fellow of the Hungarian Academy of Sciences, which is gratefully acknowledged. M. J. and M. N. D. S. C. acknowledge financial support from Fundação para a Ciência e a Tecnologia – Portugal, through project PTDC/EQU-FTT/104195/2008.

References

[1] McFearin, C. L.; Beaman, D. K.; Moore, F. G.; Richmond, G. L. *J. Phys. Chem. C* **2009**, *113*, 1171.

[2] Benjamin, I. *Annu. Rev. Phys. Chem.* **1997**, *48*, 407.

[3] Schlossman, M. L. *Curr. Opin. Colloid Interface Sci.* **2002**, *7*, 235.

[4] Rowlinson, J; Widom, B. *Molecular Theory of Capillarity*; Clarendon Press: Oxford, 1982.

[5] Buff, F.; Lovett, R.; Stillinger, F. *Phys. Rev. Lett.* **1965**, *15*, 621.

[6] Willard, A. P.; Chandler, D. *J. Phys. Chem. B*, **2010**, *114*, 1954.

[7] Stillinger, F. H. *J. Chem. Phys.* **1982**, *76*, 1087.

[8] Chacón, E.; Tarazona, P. *Phys. Rev. Lett.* **2003**, *91*, 166103.

[9] Jorge, M.; Cordeiro, M. N. D. S. *J. Phys. Chem. C* **2007**, *111*, 17612.

[10] Pandit, S. A.; Bostick, D.; Berkowitz, M. L. *J. Chem. Phys.* **2003**, *119*, 2199.

[11] Chowdhary, J.; Ladanyi, B. M. *J. Phys. Chem. B* **2006**, *110*, 15442.

[12] Jorge, M.; Jedlovszky, P.; Cordeiro, M. N. D. S. *J. Phys. Chem. C* **2010**, *114*, 11169.

[13] Tarazona, P.; Chacón, E.; *Phys. Rev. B* **2004**, *70*, 235407.

[14] Chacón, E.; Tarazona, P.; *J. Phys.: Condens. Matter* **2005**, *17*, S3493.

[15] Chacón, E.; Tarazona, P.; Alejandre, J.; *J. Chem. Phys.* **2006**, *125*, 014709.

[16] Bresme, F.; Chacón, E.; Tarazona, P.; *Phys. Chem. Chem. Phys*. **2008**, *10*, 4704.

[17] Chacón, E.; Fernández, E. M.; Duque, D.; Delgado-Buscalioni, R.; Tarazona, P.; *Phys. Rev. B* **2009**, *80*, 195403.

[18] Jorge, M.; Cordeiro, M. N. D. S.; *J. Phys. Chem. B* **2008**, *112*, 2415.

[19] Pártay, L. B.; Hantal, G.; Jedlovszky, P.; Vincze, A.; Horvai, G.; *J. Comput. Chem.* **2008**, *29*, 945.

[20] Pártay, L. B.; Horvai, G.; Jedlovszky, P.; *Phys. Chem. Chem. Phys*. **2008**, *10*, 4754.

[21] Lindahl, E.; Hess, B.; van der Spoel, D. *J. Mol. Mod.* **2001**, *7*, 306.

[22] Berendsen, H. J. C.; Postma, J. P. M.; DiNola, A.; Haak, J. R. *J. Chem. Phys.* **1984**, *81***,** 3684.

[23] Jorgensen, W. L.; Chandrashekar, J.; Madura, J. D.; Impey, R.; Klein, M. L. *J. Chem. Phys.* **79,** *926* (1983).

[24] Miyamoto, S.; Kollman, P. A. *J. Comput. Chem.* **1992**, *13***,** 952.

[25] McDonald, I. R.; Bounds, D. G.; Klein, M. L. *Mol. Phys.* **1982**, *45*, 521.

[26] Ryckaert, J. P.; Ciccotti, G.; Berendsen, H. J. C. *J. Comput. Phys* **1977**,. *23***,** 327.

[27] Essman, U.; Perela, L.; Berkowitz, M. L.; Darden, T.; Lee, H.; Pedersen, L. G. *J. Chem. Phys.* **1995**, *103*, 8577.

[28] Press, W.; Teukolsky, S.; Vetterling, W.; Flannery, B. *Numerical recipes in C*. 2 ed.; Cambridge University Press: Cambridge, 1992.

TOC GRAPHIC

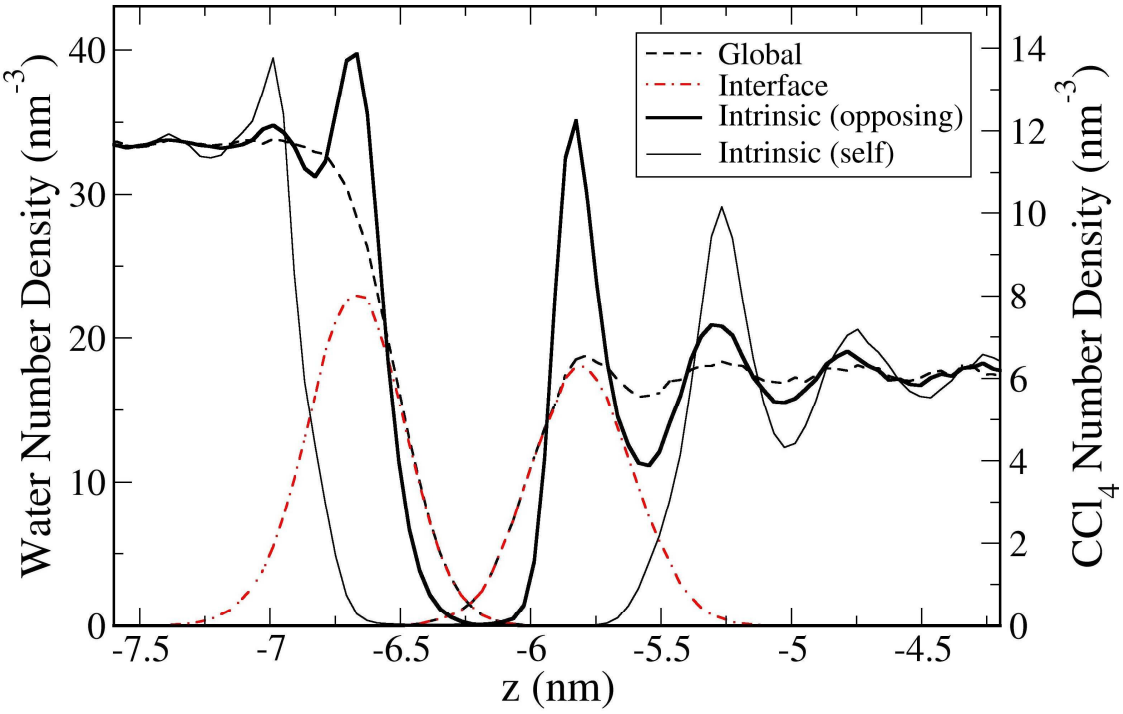
Global
Interface
Intrinsic (opposing)
Intrinsic (self)
Water Number Density (nm^{-3})
CCl_4 Number Density (nm^{-3})
z (nm)
0
10
20
30
40
0
2
4
6
8
10
12
14
-7.5
-7
-6.5
-6
-5.5
-5
-4.5